Metallaphotoredox C-O and C-N Cross-coupling using Donor-Acceptor Cyanoarene Photocatalysts

Tommaso Gandini,[a] Luigi Dolcini,[a] Lorenzo Di Leo,[a] Matthieu Fornara,[a] Alberto Bossi,[b] Marta Penconi,[b] Alberto Dal Corso,[a] Cesare Gennari*[a] and Luca Pignataro*[a]

[a] Tommaso Gandini, Luigi Dolcini, Lorenzo Di Leo, Matthieu Fornara, Dr. Alberto Dal Corso, Prof. Cesare Gennari, Prof. Luca Pignataro
Dipartimento di Chimica
Università degli Studi di Milano
Via C. Golgi, 19 – 20133 Milano (Italy)
E-mail: cesare.gennari@unimi.it
luca.pignataro@unimi.it
Homepage: https://sites.unimi.it/gennarigroup/
Twitter: @LaStatale

[b] Dr. Alberto Bossi, Dr. Marta Penconi
Istituto di Scienze e Tecnologie Chimiche "Giulio Natta" (SCITEC) del Consiglio Nazionale delle Ricerche (CNR), via Fantoli 16/15, 20138 Milano, Italy
SmartMatLab Center, via C. Golgi 19, 20133 Milano, Italy

Supporting information for this article is given via a link at the end of the document.

Abstract: Herein we report a study on the use of donor-acceptor cyanoarenes as photocatalysts for C-O and C-N coupling reactions promoted by nickel. We found that some of these stable and readily available organic compounds can replace the precious metal photocatalysts originally employed in these methodologies. After reaction optimization, the application scope of the best performing dyes was investigated and found to cover several nucleophiles (alcohols and amines) and aryl bromides. Control experiments, fluorescence quenching studies and examination of yield trends suggest that both etherification and amination probably proceed via a dark Ni^{I}/Ni^{III}-catalytic cycle initiated and sustained by a photoredox cycle involving the organic photocatalysts.

Introduction

Originally developed as OLED emitters,[1] donor-acceptor (D-A) cyanoarenes have risen to one of the most important classes of organic dyes for applications in (metalla)photoredox catalysis,[2] owing to several attractive features. Firstly, they possess spatially separated frontier molecular orbitals enabling the thermally-activated delayed fluorescence (TADF) mechanism,[3] which ensures relatively long excited state lifetimes (1-10 µs range for the delayed component). Additionally, as shown by Zhang,[4] Zeitler[5] and others,[6] their modular structure allows to tune the photophysical and redox properties by varying number, type and position of the donor substituents connected to the cyanoarene core. Finally, unlike many other organic dyes, D-A cyanoarenes are robust neutral molecules, mostly accessible in one step from cheap commercial compounds and easy to purify by either recrystallization or chromatography.

Dual nickel/photoredox catalysis,[7] introduced by the seminal contributions of Doyle-MacMillan[8] and Molander,[9] is one of the main areas in which D-A cyanoarenes have been successfully applied to replace the expensive Ru- and Ir-photocatalysts. Perhaps surprisingly, however, most reported applications are in C-C coupling reactions,[4,5,6e,10,11,12] whereas only a few applications to C-O[13] and C-S bond formation[14] are known, and C-N coupling is yet substantially uncovered.[15]

Herein, we report the use of D-A cyanoarenes as photocatalysts to promote the nickel-catalyzed cross-coupling of amines and alcohols to aryl bromides.

Results and Discussion

We synthesized a small library of D-A cyanoarenes (Figure 1 A) in one step following the protocols developed by Zhang (**4CzIPN**),[4] Zeitler (**3CzClIPN**, **3DPAFIPN**, **5CzBN**, **3DPA2FBN**),[5] Wickens (**4DPAIPN**)[16] and Bergens (**3CzFIPN**).[17]

The organic dyes were screened in two Ni-catalyzed cross-coupling reactions between an aryl bromide and, respectively, *n*-hexanol (Figure 1 B) and pyrrolidine (Figure 1 C) under blue light irradiation – i.e., similar conditions to the ones adopted by MacMillan and co-workers in the presence of Ir-photocatalysts.[18] Delightfully, high yields were obtained in both reactions with some D-A cyanoarenes, the best performing ones being different in C-O and in C-N coupling. For each type of cross-coupling we carried out reaction conditions optimization, assessment of substrate scope, and preliminary mechanistic investigation.

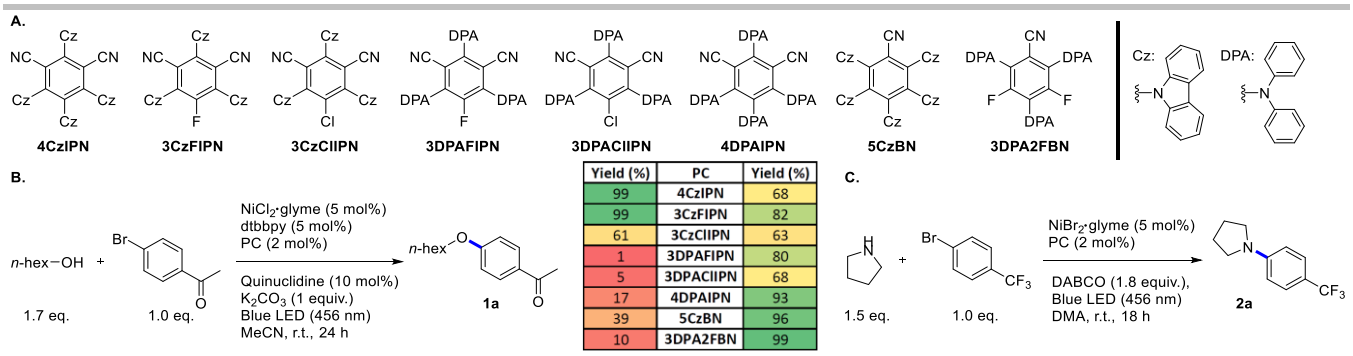

Yield (%)	PC	Yield (%)
99	4CzIPN	68
99	3CzFIPN	82
61	3CzClIPN	63
1	3DPAFIPN	80
5	3DPAClIPN	68
17	4DPAIPN	93
39	5CzBN	96
10	3DPA2FBN	99

Figure 1. A. D-A cyanoarene dyes employed in the present study. B. Screening of the photocatalysts (PCs) in a model C-O coupling reaction. C. Screening of the PCs in a model C-N coupling reaction. Before visible light irradiation, the reaction mixture was subjected to three freeze/thaw cycles, backfilling with dry nitrogen. Yields were determined by ^{1}H NMR using 1,3,5-trimethoxybenzene as internal standard. dtbbpy = 4,4'-di-*tert*-butyl-2,2'-dipyridyl.

Table 1. Control experiments and optimization of C-O coupling.[a]

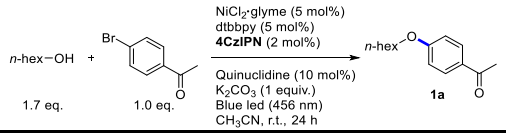

#	Deviation from the conditions above	Yield (%)
1	None	99
2	No light	0
3	No **4CzIPN**	0
4	No $NiCl_2$·glyme	0
5	No ligand	0[b]
6	No quinuclidine	trace
7	Run under air	trace
8	TMP[c] (2 equiv.) instead of K_2CO_3/quinuclidine	92
9	Acetone instead of CH_3CN	98
10	DMF instead of CH_3CN	93
11	DMA instead of CH_3CN	91
12	DABCO instead of quinuclidine	0
13	TEA instead of quinuclidine	trace
14	1.3 equiv. *n*-hexanol	94
15	4,4'-dmbpy[d] instead of dtbbpy	94
16	**4CzIPN** / $NiCl_2$·glyme / 4,4'-dmbpy (1 mol% each)	93
17	**4CzIPN** / $NiCl_2$·glyme / 4,4'-dmbpy (0.5 mol% each)	91

[a] Before visible light irradiation, the reaction mixture was subjected to three freeze/thaw cycles, backfilling with dry nitrogen. Yields were determined by ^{1}H NMR using 1,3,5-trimethoxybenzene as internal standard; dtbbpy = 4,4'-di-*tert*-butyl-2,2'-dipyridyl. [b] Acetophenone formation detected (51% yield). [c] TMP = 2,2,6,6-tetramethylpiperidine. [d] 4,4'-dmbpy = 4,4'-dimethyl-2,2'-dipyridyl.

Some results of the C-O coupling optimization, using the reaction between *n*-hexanol and 4-bromoacetophenone as model, are shown in Table 1 (see the Supporting Information for additional data). Experiments carried out in the absence of a single component show that light, photocatalyst, $NiCl_2$·glyme, bipyridine ligand and quinuclidine are all indispensable ingredients (Table 1, entries 2-6). Working under air with non-degassed solvents determined a substantial drop of the yield, with only traces of **1a** formed (entry 7). Replacing K_2CO_3 and quinuclidine (Q) with 2 equiv. of 2,2,6,6-tetramethylpiperidine (TMP), featuring a redox potential similar to quinuclidine (E ($TMP^{\bullet+}$/TMP) = 1.00 V vs. SCE;[19] E ($Q^{\bullet+}$/Q) = 1.1 V vs. SCE[20]) led to a slightly decreased but still good yield (entry 8). High yields were obtained in several polar solvents, such as acetone, DMF and DMA (entries 9-11). While dtbbpy can be replaced with other bipyridines such as 4,4'-dmbpy (entry 15), quinuclidine is the only tertiary amine which allows product formation (entries 12-13 vs. 1). Use of a lesser excess of *n*-hexanol led to a slightly lower yield (entry 14 vs. 1). Notably, the loading of nickel catalyst and photocatalyst can be lowered to 0.5 mol% without significantly eroding the yield (entries 16-17 vs. 15). Finally, using light of different wavelengths within the 390-456 nm range gave essentially the same results (see the Supporting Information). This is not surprising because, from the measured extinction coefficients (see Table S2 in the Supporting Information), we infer that, at the PC concentration used in the photocatalytic experiments, strong absorption should be ensured for all dyes even at λ = 456 nm.

With the two best performing dyes, i.e. **4CzIPN** and **3CzFIPN**, we investigated the C-O coupling scope obtaining the results shown in Scheme 1 (for each product only the best result is shown, see Table S12 for more data). Several primary alcohols, except the poorly nucleophilic 2,2,2-trifluoroethanol, gave high yields in the coupling to 4-bromoacetophenone (Scheme 1 A). Secondary and benzylic alcohols were also found to be competent nucleophiles, whereas no product formation was detected with tertiary alcohols, phenols and water (Scheme 1 C). Electron neutral and electron poor aryl bromides and heteroaryl bromides, with the exception of sterically hindered *ortho*-substituted substrates (Scheme 1 C), reacted smoothly with 1-hexanol (Scheme 1 B). The electron rich bromides were found less reactive, giving lower yields, whereas benzylic bromides and aryl chlorides failed at all to react in C-O coupling under our experimental conditions (Scheme 1 C).

As **3CzFIPN** is the only D-A cyanoarene of the library used in this study whose photo- and electrochemical properties had not been reported, we studied them obtaining the data shown in Table 2 (see the Supporting Information for key photo- and electrochemical parameters of all the library).

Table 2. Photo- and electrochemical parameters of dye **3CzFIPN**.

$E_{0,0}$	2.70 eV	$E_{1/2}$ ($PC^*/PC^{\bullet-}$)	1.59 V[a]
Prompt fluorescence lifetime (τ_p)	7.2 ns	E_{onset} ($PC^{\bullet+}/PC^*$)	-1.06 V[a]
Delayed fluorescence lifetime (τ_d)	760 ns	E_{onset} ($PC^{\bullet+}/PC$)	1.64 V[a]
ε at 456 nm	621 M^{-1} cm^{-1}	$E_{1/2}$ ($PC/PC^{\bullet-}$)	-1.11 V[a]

[a] Electrochemical potentials are referenced to the saturated calomel electrode (SCE). $E_{1/2}$, for reversible or quasi reversible processes, indicates the half-wave potential; E_{onset}, for irreversible processes, is referred to the potential which is at 5% of the peak height.

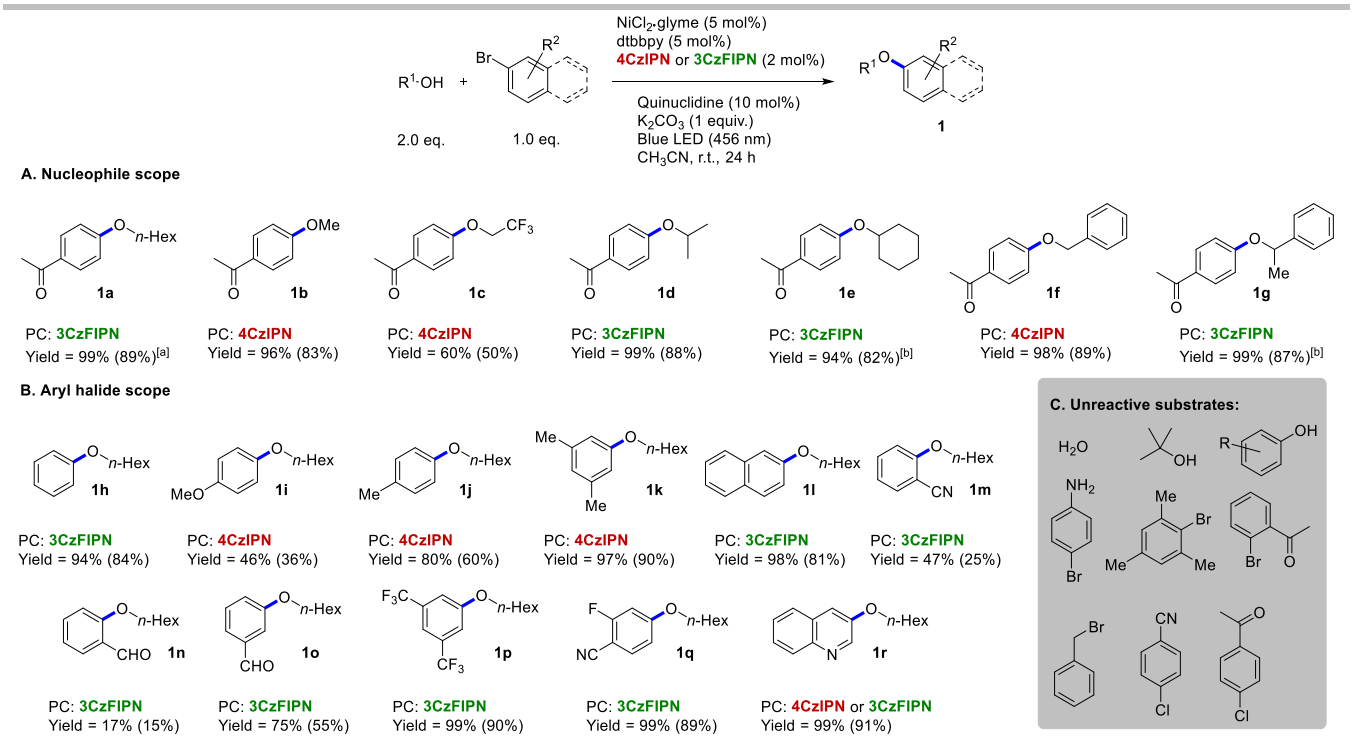

Scheme 1. Substrate scope investigation in C-O coupling (data obtained with the best performing PC are shown). A. Nucleophile scope. B. Aryl halide scope. C. Unreactive substrates (yield < 5%). Before visible light irradiation, the reaction mixture was subjected to three freeze/thaw cycles, backfilling with dry nitrogen. Isolated yields are shown in brackets, whereas NMR yields (outside brackets) were determined by ^{1}H NMR analysis of the reaction crudes using 1,3,5-trimethoxybenzene as internal standard. [a] 1.7 equiv. of alcohol used. [b] 4 equiv. of alcohol used.

Yields of the model C-O coupling reaction (Figure 1 B) and photo/electrochemical properties of the dyes were confronted to identify possible trends (see also the Supporting Information).

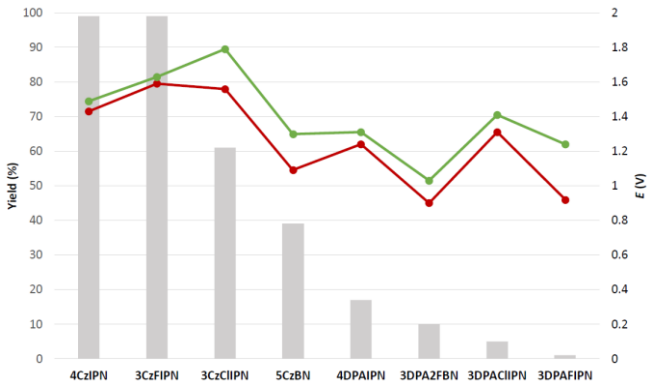

Figure 2. Synopsis of C-O coupling yields (grey histograms) and PCs' oxidation potentials *E* (PC*/PC$^{\bullet-}$) (-●-) and *E* (PC$^{\bullet+}$/PC) (-■-). Electrochemical potentials are referenced to SCE.

Remarkably we found that, as general trend, the C-O coupling yields grow with the increasing oxidizing power of the photocatalyst [i.e., high positive *E* (PC*/PC$^{\bullet-}$) and *E* (PC$^{\bullet+}$/PC) values], as shown in Figure 2. This leads to hypothesize a photoredox mechanism featuring a critical oxidation step performed by the catalyst.[21] For their metallaphotoredox etherification employing Ir-photocatalysts,[8b] MacMillan and co-workers proposed a Ni^0/Ni^{II}/Ni^{III}/Ni^I mechanism where the Ni^{II} → Ni^{III} oxidation is characterized by relatively low-demanding potentials: $E_{1/2}$ (Ni^{III}/Ni^{II}) = 0.83 V vs. SCE for (dtbppy)Ni^{II}(2,4-bis(CF$_3$)C$_6$H$_3$)(OCH$_2$CF$_3$),[8b] and 0.70 V vs. SCE for Ni^{II}(Mes)(OMe)(bpy).[7h] In contrast, the oxidation of quinuclidine (Q) is less easy, since the potential of the Q$^{\bullet+}$/Q redox couple is quite strongly positive [*E* (Q$^{\bullet+}$/Q) = 1.1 V vs. SCE in CH$_3$CN],[20] which may indicate a pivotal role of this oxidation step during the reaction. Quinuclidine oxidation may be performed by the photocatalyst either in its excited state (reductive quenching of PC*) or in the radical cation form (PC$^{\bullet+}$) generated from the

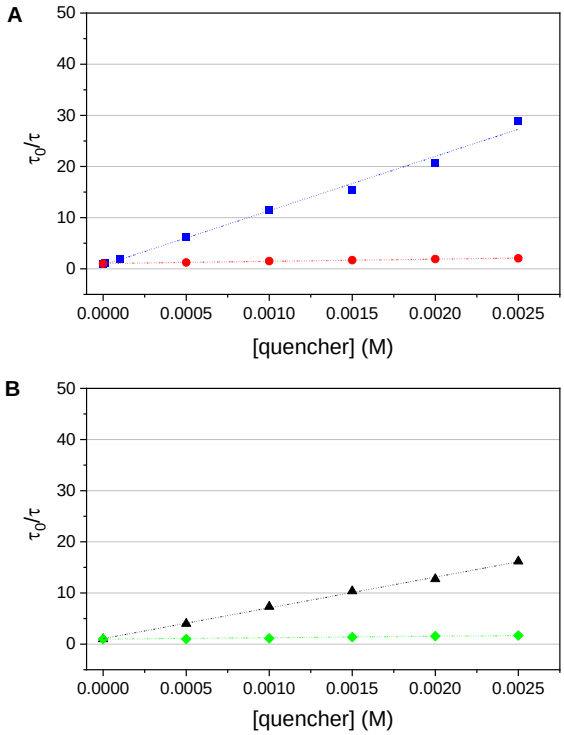

Figure 3. Stern-Volmer plots of delayed lifetimes (excitation at 375 nm, emission at 560 nm) in Ar-degassed acetonitrile. A. **4CzIPN** (0.01 mM) in the presence of quinuclidine (■) and NiCl$_2$(dtbbpy) (●). B. **3CzFIPN** (0.01 mM) in the presence of quinuclidine (▲) and NiCl$_2$(dtbbpy) (♦).

oxidative quenching of PC*. We ran Stern-Volmer fluorescence quenching experiments with both **4CzIPN** (Figure 3 A) and **3CzFIPN** (Figure 3 B) to ascertain which is the preferential photocatalyst de-excitation route among the most likely ones, i.e. by quinuclidine oxidation (reductive quenching) or by $NiCl_2$(dtbbpy) reduction (oxidative quenching). The former scenario is the most likely in both cases, as PC* is quenched by quinuclidine more strongly than by $NiCl_2$(dtbbpy).

This finding seems in agreement with the mechanism proposed by Nocera and co-workers for Ni/photoredox aryl bromide etherification (see Scheme 2),[22] in which a photoredox catalytic cycle involving PC* quenching by quinuclidine has the role to activate and sustain a dark Ni^{I}/Ni^{III} cross-coupling cycle that is otherwise deactivated by side reactions: the radical anion $PC^{\bullet-}$, generated by quinuclidine oxidation, reduces $Ni^{II}Cl_2$(dtbbpy) to the catalytically active Ni^{I} complex [we measured, for $Ni^{II}Cl_2$(dtbbpy), E (Ni^{II}/Ni^{I}) = -0.84 V as shown in the Supporting Information].

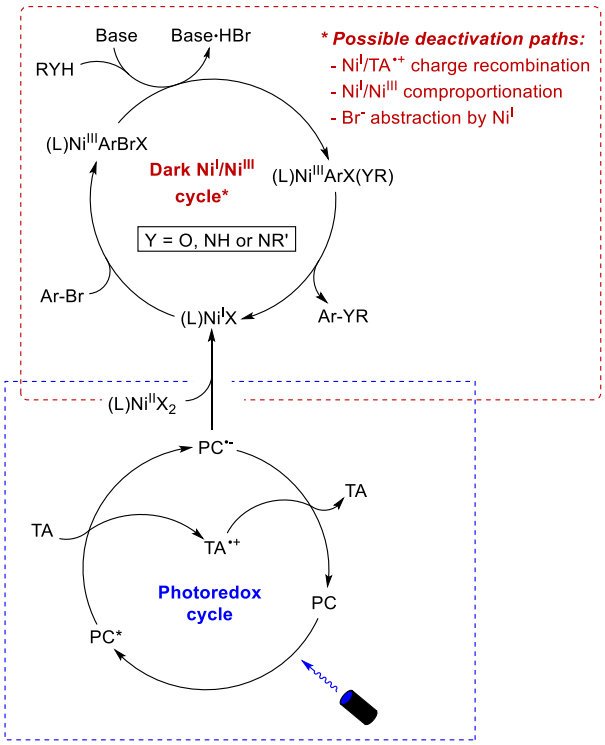

Scheme 2. Mechanism proposed for the Ni-catalyzed C-O and C-N cross-coupling promoted by D-A cyanoarenes. PC = photocatalyst; TA (tertiary amine) = quinuclidine (in C-O coupling) or DABCO (in C-N coupling).

Some results of the C-N coupling optimization are shown in Table 3, while additional data can be found in the Supporting Information. We found that the reaction does not proceed in the absence of a nickel source (Table 3, entry 4), and several different complexes/salts can promote it (entries 14-16). Notably, identical results are obtained in the presence and in the absence of a bipyridine ligand (entry 16 vs. 15). Use of polar solvents different from DMA gave slightly decreased but still satisfactory yields (entries 7-9). To our surprise, the reaction proceeds also in the dark (entry 2) and in the absence of photocatalyst (entry 3), albeit in low yield. In sharp contrast with etherification, a good yield of C-N coupling product was obtained when the reaction was run under air (entry 6). Replacement of DABCO with other amine bases/reductants led to a decrease of yield (Table 3, entries 12-13 vs. 1), as did reduction of the stoichiometric amount (entries 10-11 vs. 1). Surprisingly, however, the reaction proceeded even in the absence of DABCO, affording the product in 62% yield (entry 5).

Under the optimized conditions the substrate scope of the C-N cross-coupling was investigated using **3DPA2FBN** and **5CzBN**, and the best obtained results are shown in Scheme 3 (see Table S18 for additional data). Several N-nucleophiles were coupled to 4-bromobenzotrifluoride (Scheme 3 A), and moderate to good yields were achieved with primary and secondary amines.

Table 3. Control experiments and optimization of C-N coupling.[a]

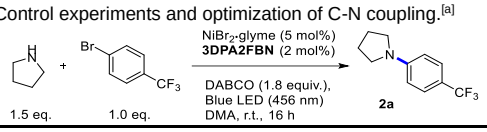

#	Deviation from the conditions above	Yield (%)
1	None	99
2	No light	26
3	No **3DPA2FBN**	8
4	No $NiBr_2$·glyme	0
5	No DABCO	62
6	Run under air	95
7	DMF instead of DMA	95
8	CH_3CN instead of DMA	92
9	THF instead of DMA	50
10	1 equiv. instead of 1.8 equiv. DABCO	63
11	1.5 equiv. instead of 1.8 equiv. DABCO	73
12	Quinuclidine instead of DABCO	54
13	TEA instead of DABCO	31
14	$Ni(cod)_2$ instead of $NiBr_2$·glyme	99
15	$NiCl_2$·glyme instead of $NiBr_2$·glyme	85
16	$NiCl_2$(dtbbpy) instead of $NiBr_2$·glyme	85

[a] Before visible light irradiation, the reaction mixture was subjected to three freeze/thaw cycles. Yields were determined by ^1H NMR using 1,3,5-trimethoxybenzene as internal standard.

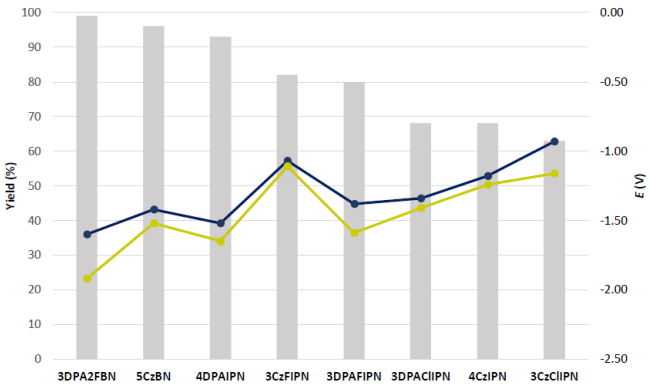

Figure 4. Synopsis of C-N coupling yields (grey histograms) and PCs' reduction potentials E ($PC/PC^{\bullet-}$) (-●-) and E ($PC^{\bullet+}/PC^*$) (-■-). Electrochemical potentials are referenced to SCE.

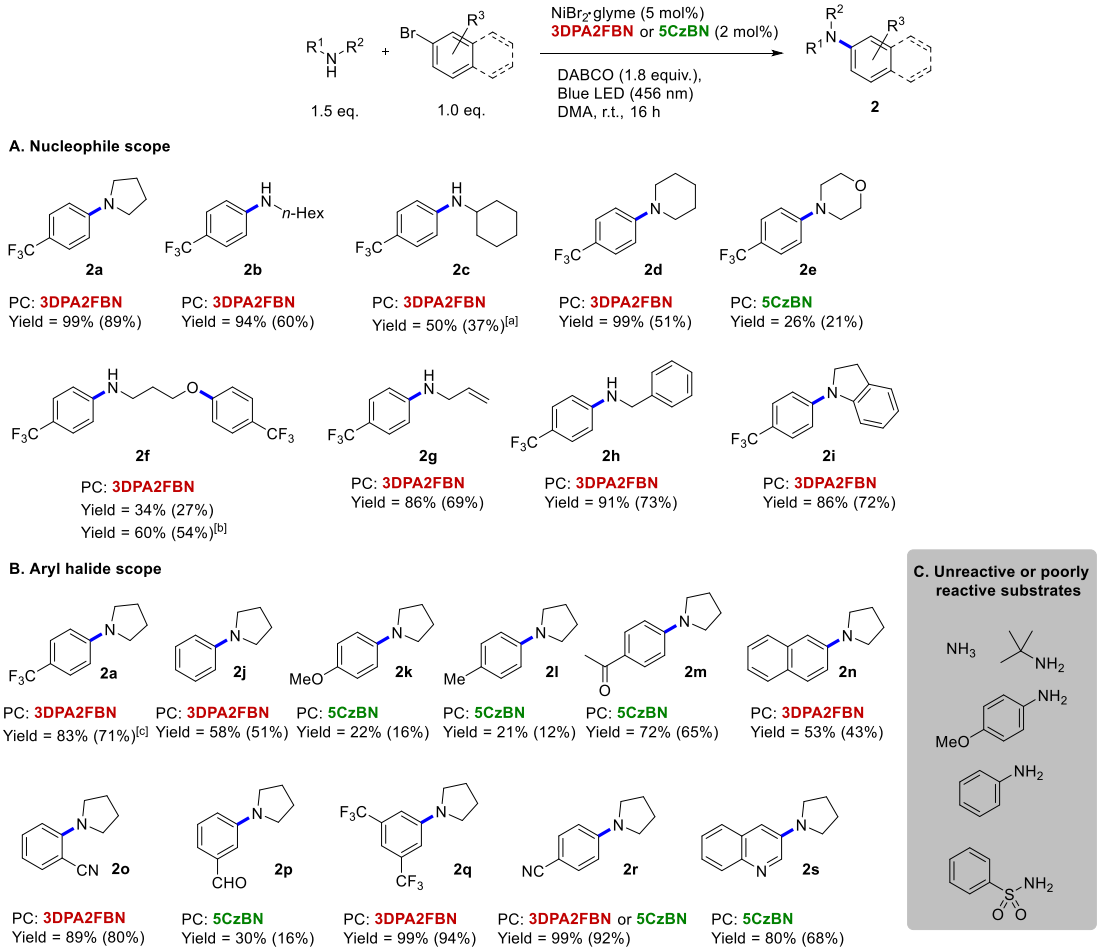

Scheme 3. Substrate scope investigation in C-N coupling. A. Nucleophile scope. B. Aryl halide scope. C. Unreactive substrates (yield < 5%). Isolated yields are shown in brackets, whereas NMR yields (outside brackets) were determined by ^{1}H NMR analysis of the reaction crudes using 1,3,5-trimethoxybenzene as internal standard. [a] 3 equiv. of amine used. [b] 3-aminopropanol (1 equiv.); 4-bromobenzotrifluoride (2 equiv.). [c] 4-Chlorobenzotrifluoride used instead of 4-bromobenzotrifluoride.

Notable exceptions to this trend are morpholine – which gave low yield in sharp contrast to piperidine – and aniline, much less reactive than the structurally related indoline. Benzenesulfonamide also gave the coupling product in very low yield (< 5%, Scheme 3 C). Using pyrrolidine as nucleophile, the scope of aryl bromides was assessed (Scheme 3 B). The electron poor aryl bromides formed the corresponding products – including *ortho* substituted **2o** – in good yields, whereas the electron neutral substrates were slightly less reactive. Following this trend, the substrates possessing an electron donor substituent gave the cross-coupling products **2k** and **2l** in low yield (22% and 21%, respectively, with **5CzBN**). Remarkably, we found that also 4-chlorobenzotrifluoride reacts with pyrrolidine to afford compound **2a** in good yield (71%, Scheme 3 A), thus showing that the methodology is potentially suitable for aryl chloride substrates.

Contrary to what observed for C-O coupling, no correlation between yields and PC's oxidizing power was observed for the amination reaction (see the Supporting Information). This finding is consistent with a photoredox mechanism[21] where the PC oxidizes DABCO (D), which has lower potential than quinuclidine (Q) used in C-O coupling (E ($D^{\bullet+}$/D) = 0.71 V[23] vs. SCE; E ($Q^{\bullet+}$/Q) = 1.1 V vs. SCE[20]). The oxidation of DABCO, which may involve either the photoexcited photocatalyst (reductive quenching of PC*) or its radical cation (reduction of $PC^{\bullet+}$, deriving from oxidative quenching of PC*), is not as critical as quinuclidine oxidation in C-O coupling. Instead, we found that the most reducing dyes [i.e., with strongly negative E ($PC^{\bullet+}$/PC*) and E ($PC/PC^{\bullet-}$) values] gave the best yields in C-N coupling, as can be seen in Figure 4. Although control experiments showed that the model reaction proceeds also in the absence of DABCO (see Table 3, entry 5), it should be noted that the nucleophilic amine itself is also able to reduce the photocatalyst [e.g., E (pyrrolidine$^{\bullet+}$/pyrrolidine) = 0.85 V vs. SCE in CH_3CN].[24]

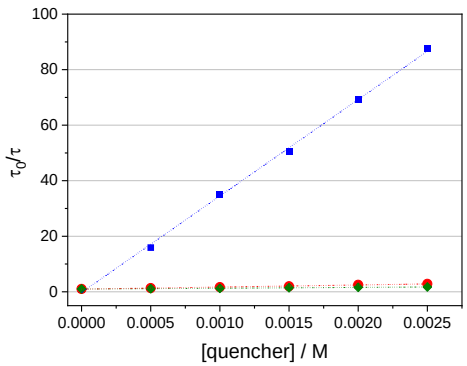

Figure 5. Stern-Volmer plot of delayed lifetimes (excitation at 375 nm, emission at 560 nm) of **5CzBN** in the presence of DABCO (■), piperidine (♦) and 1:4 $NiBr_2$·glyme/piperidine (●) in Ar-degassed DMA (*N*,*N*-dimethylacetamide).

We undertook experiments to identify the preferential de-excitation pathway of PC*. **3DPA2FBN** was not used for these studies because we found that, under visible light irradiation (456 nm), it is gradually transformed into byproducts which were identified by UPLC-MS (see the Supporting Information). From

time-resolved Stern-Volmer experiments carried out with **5CzBN** (Figure 5) it emerged that DABCO is by far the most effective quencher of the photocatalyst. This finding is consistent with a reductive quenching of PC* taking place, as postulated on the basis of the redox potentials.

Based on these results, and considering that the model reaction gives some conversion (yet very low) also in the absence of light or photocatalyst (see Table 3, entries 2-3), we infer that also our C-N coupling probably proceeds via a 'dark' Ni^{I}/Ni^{III} catalytic cycle triggered and sustained by a photocatalytic cycle involving DABCO or other reductants present in the reaction environment (see Scheme 2). This mechanism is similar to the one proposed by MacMillan and co-workers for the same transformation run in the presence of Ir photocatalysts.[23] However, a mechanistic scenario involving a $Ni^{0}/Ni^{II}/Ni^{III}/Ni^{I}$ catalytic cycle[18] cannot be excluded with the data in our possess.

Conclusion

Using a library of seven D-A cyanoarenes, we have investigated their catalytic activity in aryl bromide etherification and amination, that had previously been carried out mostly with precious metal photocatalysts. In both C-O and C-N coupling, several dyes have shown a good catalytic activity and a sufficiently wide application scope, allowing to establish a truly base metal catalytic methodology of potential preparative utility. Examination of the redox potentials of reagents and photocatalysts, yield trends and Stern-Volmer experiments led us to propose, for both types of reaction, a mechanism in which a photoredox catalytic cycle initiates and sustains a Ni^{I}/Ni^{III} cycle involving oxidative addition followed by reductive elimination.

Experimental Section

General remarks

The catalytic tests were performed in septum-sealed 10 mL microwave vials. Irradiation was performed using Kessil PR160L lamps of the specified wavelength while cooling with a fan to dissipate the heat produced by the lamp. Analytical thin layer chromatography (TLC) was carried out using commercial silica gel plates, spots were detected with UV light and revealed either with cerium-ammonium molybdate or potassium permanganate alkaline solution. Flash column chromatography was performed using silica gel (60 Å, particle size 40-64 μm) as stationary phase, following the procedure by Still and co-workers.[25] ^{1}H NMR spectra were recorded on a 400 MHz spectrometer.

General procedure for C-O cross-coupling

To a vial containing a stirring bar, the aryl halide (0.5 mmol, 1.0 equiv.), potassium carbonate (69.8 mg, 0.5 mmol, 1 equiv.), photocatalyst (0.025 mmol, 0.05 equiv.) and quinuclidine (5.73 mg, 0.05 mmol, 0.1 equiv.) were added. The vial was sealed with a cap with septum and purged with nitrogen for 2 min, then freshly distilled acetonitrile was added (1 mL). A solution of $NiCl_2$·glyme (5.61 mg, 0.025 mmol, 0.05 equiv.) and 4,4'-di-*tert*-butyl-2,2'-dipyridyl (6.85 mg, 0.025 mmol, 0.05 equiv.) in freshly distilled acetonitrile (2 mL) was sonicated and added to the vial. At last, the alcohol (0.85-2.0 mmol, 1.7-4 equiv.) was added, and the reaction mixture was subjected to three freeze-pump-thaw cycles, backfilling with dry nitrogen. The magnetically stirred reaction was run at room temperature for 24 h under irradiation with a blue LED lamp (λ = 456 nm; distance between lamp and vial(s): 5 cm; a fan was used to dissipate the heat generated by the lamp). 1,3,5-Trimethoxybenzene (42.1 mg, 0.25 mmol, 0.5 equiv.) – the internal standard for ^{1}H NMR analysis – was added, and the reaction mixture was stirred for 5 min. Water (10 mL) was added and then the mixture was extracted three times with ethyl acetate. The combined organic extracts were washed with brine, dried (Na_2SO_4) and then concentrated. The crude mixture was analyzed by ^{1}H NMR and then purified by flash column chromatography on silica gel to afford the desired product.

General procedure for C-N cross-coupling

To a vial containing a stirring bar the photocatalyst (0.011 mmol, 0.02 equiv.) and DABCO (111.7 mg, 0.976 mmol, 1.8 equiv.) were added. The vial was sealed and purged with nitrogen for 2 min, then dry DMA was added (1.0 mL). The aryl bromide (0.542 mmol, 1 equiv.), the amine (0.813 mmol, 1.5 equiv.) and a solution of $NiBr_2$·glyme (8.33 mg, 0.027 mmol, 0.05 equiv.) in DMA (1 mL) were added. The reaction mixture was subjected to three freeze-pump-thaw cycles, backfilling with dry nitrogen. The magnetically stirred reaction was run at room temperature for 16 h under irradiation with a blue LED lamp (λ = 456 nm; distance between lamp and vial(s): 5 cm; a fan was used to dissipate the heat generated by the lamp). 1,3,5-Trimethoxybenzene (45.6 mg, 0.271 mmol, 0.5 equiv.) – the internal standard for ^{1}H NMR analysis – was added, and the reaction mixture was stirred for 5 min. The reaction mixture was filtered through a plug of silica (washing with Et_2O), then the volatiles were evaporated and ^{1}H NMR analysis of the crude product was performed. The reaction product was purified by flash column chromatography on silica gel.

Acknowledgements

L. Pignataro thanks 'Piano di Sostegno alla Ricerca 2021' (Dipartimento di Chimica, Università degli Studi di Milano) and Ministero dell'Università e della Ricerca (PRIN 2017 project no. 20174SYJAF, "Raising up Catalysis for Innovative Developments" - SURSUMCAT") for financial support.

Keywords: metallaphotoredox catalysis • nickel • donor-acceptor cyanoarenes • cross-coupling • organic dyes

[1] H. Uoyama, K. Goushi, K. Shizu, H. Nomura, C. Adachi, *Nature* **2012**, *492*, 234-238.
[2] For reviews on (metalla)photoredox catalysis with organic dyes, see: a) N. A. Romero, D. A. Nicewicz, *Chem. Rev.* **2016**, *116*, 10075-10166; b) T.-Y. Shang, L.-H. Lu, Z. Cao, Y. Liu, W.-M. He, B. Yu, *Chem. Commun.* **2019**, *55*, 5408-5419; c) A. Gualandi, M. Anselmi, F. Calogero, S. Potenti, E. Bassan, P. Ceroni, P. G. Cozzi, *Org. Biomol. Chem.* **2021**, *19*, 3527-3550.
[3] For reviews on TADF compounds in catalysis, see: M. A. Bryden, E. Zysman-Colman, *Chem. Soc. Rev.* **2021**, *50*, 7587-7680.
[4] J. Luo, J. Zhang, *ACS Catal.* **2016**, *6*, 873-877.
[5] E. Speckmeier, T. G. Fischer, K. Zeitler, *J. Am. Chem. Soc.* **2018**, *140*, 15353-15365.
[6] a) Y. J. Cho, K. S. Yook, J. Y. Lee, *Adv. Mater.* **2014**, *26*, 6642-6646; b) R. Ishimatsu, T. Edura, C. Adachi, K. Nakano, T. Imato, *Chem. Eur. J.* **2016**, *22*, 4889-4898; c) Y. Im, M. Kim, Y. J. Cho, J.-A. Seo, K. S. Yook, J. Y. Lee, *Chem. Mater.* **2017**, *29*, 1946-1963; d) Y. Im, M. Kim, Y. J. Cho, J.-A. Seo, K. S. Yook, J. Y. Lee, *Chem. Mater.* **2017**, *29*, 1946-1963; e) M. Garreau, F. Le Vaillant, J. Waser, *Angew. Chem. Int. Ed.* **2019**, *58*, 8182-8186; *Angew. Chem.* **2019**, *131*, 8266-8270.
[7] For relevant reviews, see: a) M. D. Levin, S. Kim, F. D. Toste, *ACS Cent. Sci.* **2016**, *2*, 293-301; b) Y.-Y. Gui, L. Sun, Z.-P. Lu, D.-G. Yu, *Org. Chem. Front.* **2016**, *3*, 522-526; c) J. Twilton, C. Le, P. Zhang, M. H. Shaw, R. W. Evans, D. W. C. MacMillan, *Nat. Rev. Chem.* **2017**, *1*, 0052; d) J. K. Matsui, S. B. Lang, D. R. Heitz, G. A. Molander, *ACS Catal.* **2017**, *7*, 2563-2575; e) C. Zhu, H. Yue, J. Jia, M. Rueping, *Angew. Chem. Int. Ed.* **2021**, *60*, 17810-17831; *Angew. Chem.* **2021**, *133*, 17954-17975; f) Z. Ye, Y.-M. Lin, L. Gong, *Eur. J. Org. Chem.* **2021**, 5545-5556; g) A. Gualandi, M. Anselmi, F. Calogero, S. Potenti, E. Bassan, P. Ceroni, P. G. Cozzi, *Org. Biomol.*

Chem. **2021**, *19*, 3527-3550; h) O. S. Wenger, *Chem. Eur. J.* **2021**, *27*, 2270-2278; i) A. Y. Chan, I. B. Perry, N. B. Bissonnette, B. F. Buksh, G. A. Edwards, L. I. Frye, O. L. Garry, M. N. Lavagnino, B. X. Li, Y. Liang, E. Mao, A. Millet, J. V. Oakley, N. L. Reed, H. A. Sakai, C. P. Seath, D. W. C. MacMillan, *Chem. Rev.* **2022**, *122*, 1485-1542.

[8] a) Z. Zuo, D. T. Ahneman, L. Chu, J. A. Terrett, A. G. Doyle, D. W. C. MacMillan, *Science* **2014**, *345*, 437-440; b) J. A. Terrett, J. D. Cuthbertson, V. W. Shurtleff, D. W. C. MacMillan, *Nature* **2015**, *524*, 330-334.

[9] J. C. Tellis, D. N. Primer, G. A. Molander, *Science* **2014**, *345*, 433-436.

[10] a) Á. Gutiérrez-Bonet, J. C. Tellis, J. K. Matsui, B. A. Vara, G. A. Molander, *ACS Catal.* **2016**, *6*, 8004-8008; b) C. Lévêque, L. Chenneberg, V. Corcé, C. Ollivier, L. Fensterbank, *Chem. Commun.* **2016**, *52*, 9877-9880; c) J. K. Matsui, G. A. Molander, *Org. Lett.* **2017**, *19*, 436-439; d) H. Huang, X. Li, C. Yu, Y. Zhang, P. S. Mariano, W. Wang, *Angew. Chem. Int. Ed.* **2017**, *56*, 1500-1505; *Angew. Chem.* **2017**, *129*, 1522-1527; e) Q.-Y. Meng, S. Wang, B. König, *Angew. Chem. Int. Ed.* **2017**, *56*, 13426-13430; *Angew. Chem.* **2017**, *129*, 13611-13615; f) Q.-Y. Meng, S. Wang, G. S. Huff, B. König, *J. Am. Chem. Soc.* **2018**, *140*, 3198-3201; g) S. O. Badir, A. Dumoulin, J. K. Matsui, G. A. Molander, *Angew. Chem. Int. Ed.* **2018**, *57*, 6610-6613; *Angew. Chem.* **2018**, *130*, 6720-6723; h) J. Yi, S. O. Badir, L. M. Kammer, M. Ribagorda, G. A. Molander, *Org. Lett.* **2019**, *21*, 3346-3351; i) J. P. Phelan, S. B. Lang, J. Sim, S. Berritt, A. J. Peat, K. Billings, L. Fan, G. A. Molander, *J. Am. Chem. Soc.* **2019**, *141*, 3723-3732; j) Y. Luo, Á. Gutiérrez-Bonet, J. K. Matsui, M. E. Rotella, R. Dykstra, O. Gutierrez, G. A. Molander, *ACS Catal.* **2019**, *9*, 8835-8842; k) T. J. Steiman, J. Liu, A. Mengiste, A. G. Doyle, *J. Am. Chem. Soc.* **2020**, *142*, 7598-7605; l) M. S. Santos, A. G. Corrêa, M. W. Paixão, B. König, *Adv. Synth. Catal.* **2020**, *362*, 2367-2372; m) M. Garbacz, S. Stecko, *Adv. Synth. Catal.* **2020**, *362*, 3213-3222; n) N. Alandini, L. Buzzetti, G. Favi, T. Schulte, L. Candish, K. D. Collins, P. Melchiorre, *Angew. Chem. Int. Ed.* **2020**, *59*, 5248-5253; *Angew. Chem.* **2020**, *132*, 5286-5291; o) R. S. Mega, V. K. Duong, A. Noble, V. K. Aggarwal, *Angew. Chem. Int. Ed.* **2020**, *59*, 4375-4379.

[11] For enantioselective examples, see: a) E. E. Stache, T. Rovis, A. G. Doyle, *Angew. Chem. Int. Ed.* **2017**, *56*, 3679-3683; *Angew. Chem.* **2017**, *129*, 3733-3737; b) C. Pezzetta, D. Bonifazi, R. W. M. Davidson, *Org. Lett.* **2019**, *21*, 8957-8961; c) H. Guan, Q. Zhang, P. J. Walsh, J. Mao, *Angew. Chem. Int. Ed.* **2020**, *59*, 5172-5177; *Angew. Chem.* **2020**, *132*, 5210-5215.

[12] For a successful application in photoredox-mediated atom transfer radical polymerization (O-ATRP), see: V. K. Singh, C. Yu, S. Badgujar, Y. Kim, Y. Kwon, D. Kim, J. Lee, T. Akhter, G. Thangavel, L. S. Park, J. Lee, P. C. Nandajan, R. Wannemacher, B. Milián-Medina, L. Lüer, K. S. Kim, J. Gierschner, M. S. Kwon, *Nat. Catal.* **2018**, *1*, 794-804.

[13] a) J. Lu, B. Pattengale, Q. Liu, S. Yang, W. Shi, S. Li, J. Huang, J. Zhang, *J. Am. Chem. Soc.* **2018**, *140*, 13719-13725; b) H. Lee, N. C. Boyer, Q. Deng, H.-Y. Kim, T. K. Sawyer, N. Sciammetta, *Chem. Sci.* **2019**, *10*, 5073-5078; c) M. González-Esguevillas, D. F. Fernández, J. A. Rincón, M. Barberis, O. de Frutos, C. Mateos, S. García-Cerrada, J. Agejas, D. W. C. MacMillan, *ACS Cent. Sci.* **2021**, *7*, 1126-1134.

[14] J. Santandrea, C. Minozzi, C. Cruché, S. K. Collins, *Angew. Chem. Int. Ed.* **2017**, *56*, 12255-12259; *Angew. Chem.* **2017**, *129*, 12423-12427.

[15] **4CzIPN** has been included in the photocatalyst screening for the sulfamidation of haloarenes, although the photocatalyst of choice is an Ir-complex: a) J. M. Blackburn, A. L. Gant Kanegusuku, G. E. Scott, J. L. Roizen, *Org. Lett.* **2019**, *21*, 7049-7054; b) B. Y. Park, M. T. Pirnot, S. L. Buchwald, *J. Org. Chem.* **2020**, *85*, 3234-3244.

[16] C. P. Chernowsky, A. F. Chmiel, Z. K. Wickens, *Angew. Chem. Int. Ed.* **2021**, *60*, 21418-21425; *Angew. Chem.* **2021**, *133*, 21588-21595.

[17] L. Rasu, M. Amiri, S. H. Bergens, *ACS Appl. Mater. Interfaces* **2021**, *13*, 17745-17752.

[18] For C-O coupling, see Ref. [8b]. For C-N coupling, see: E. B. Corcoran, M. T. Pirnot, S. Lin, S. D. Dreher, D. A. DiRocco, I. W. Davies, S. L. Buchwald, D. W. C. MacMillan, *Science* **2016**, *353*, 279-283.

[19] H. Ohmori, C. Ueda, K. Yamagata, M. Masui, H. Sayo, *J. Chem. Soc., Perkin Trans. 2* **1987**, 1065-1069.

[20] a) J. L. Jeffrey, J. A. Terrett, D. W. C. MacMillan, *Science* **2015**, *349*, 1532-1536; b) X. Zhang, D. W. C. MacMillan, *J. Am. Chem. Soc.* **2017**, *139*, 11353-11356.

[21] The lack of correlation between dye's $E_{0,0}$ values and reaction yields (see the Supporting Information) led us to consider an energy transfer mechanism less likely.

[22] R. Sun, Y. Qin, S. Ruccolo, C. Schnedermann, C. Costentin, D. G. Nocera, *J. Am. Chem. Soc.* **2019**, *141*, 89-93.

[23] N. A. Till, L. Tian, Z. Dong, G. D. Scholes, D. W. C. MacMillan, *J. Am. Chem. Soc.* **2020**, *142*, 15830-15841.

[24] M. Jonsson, D. D. M. Wayner, J. Lusztyk, *J. Phys. Chem.* **1996**, *100*, 17539-17543.

[25] W. C. Still, M. Kahn, A. Mitra, *J. Org. Chem.* **1978**, *43*, 2923-2925.